Available online at www.sciencedirect.com

ScienceDirect

Procedia CIRP 14 (2014) 89 – 94

www.elsevier.com/locate/procedia

6th CIRP International Conference on High Performance Cutting, HPC2014

Machinability Characteristics of Wrought and EBM CoCrMo Alloys

A. Bordin[a], A. Ghiotti[a], S. Bruschi[a]*, L. Facchini[b], F. Bucciotti[b]

[a]*Dept. Of Industrial Engineering, University of Padova, Via Venezia 1, 35131, Padova, Italy*
[b]*Eurocoating s.p.a. , Via al Dos de la Roda 60, Pergine Valsugana, Trento, Italy*

* Corresponding author. Tel.: +39 049 8276821; fax: +39 049 8276816. *E-mail address:* stefania.bruschi@unipd.it

Abstract

The Electron Beam Melting (EBM) CoCrMo alloy is currently utilized for the production of joint replacements and fixation devices thanks to its high strength, good wear and corrosion resistance, and excellent biocompatibility. Even if its use in the biomedical sector is intensive and it is usually subjected to various machining operations for the implants production after the rapid manufacturing step, the scientific literature lacks of comprehensive data about its machinability. Therefore, the objective of the paper is to investigate the machinability characteristics of the EBM CoCrMo alloy and compare it with the machinability of the wrought CoCrMo. Semi-finishing external turning tests were performed using a commercial TiAlN coated tungsten carbide insert under a traditional mineral oil and water emulsion lubricating condition. Tool wear, surface integrity, and microstructure material analysis evidenced that the EBM alloy is more difficult to machine due to a more abrasive microstructure.

Selection and peer-review under responsibility of the International Scientific Committee of the 6th CIRP International Conference on High Performance Cutting

*Keywords:*CoCrMo, Turning, Machinability, Electron Beam Melting, Tool wear

1. Introduction

CoCrMo superalloys are widely employed in the biomedical field for the production of surgical implants thanks to their high biocompatibility, mechanical and wear resistance, tribo-corrosion and fatigue resistance. Considering the femoral elements of knee replacement implants made of CoCrMo, they are commonly machined from wrought alloys, but in the recent years, additive manufacturing techniques gained a lot of interest among the biomedical companies. Among the Additive Manufacturing techniques (ALM), Electron Beam Melting (EBM) is more and more currently adopted in the production of CoCrMo surgical implants, thanks to the advantages it shows compared to the traditional process chain, mainly the possibility to reach the final shape of the product after the forming process, with improved mechanical properties and with a designed functional porous texture on its surface. Considering as an example a total knee replacement, the modular interlocking component presents the coupling surface that is not subjected to further surface treatments after machining. To shape the modular joint, usually semi-finishing external turning operations are required, and obtaining a good surface integrity is crucial for the part fretting resistance. In literature, there are very few works concerning the machinability of wrought and EBM CoCrMo superalloys, as well as technical datasheets for the choice of the machining parameters cannot be easily found. Shao [1] investigated the machinability of the Stellite 12 in dry turning finding that coated inserts showed higher tool life and cutting performances than uncoated ones, playing the feed rate the major role in tool life. Deshpande [2] applied cryogenic cooling in machining a CoCrMo superalloy, showing the improvement of the surface integrity. This paper presents the investigation of the effects of turning parameters on the machinability of two CoCrMo alloys, one formed by a traditional hot forming process and the other by the EBM technique. A commercial TiAlN coated tungsten carbide insert dedicated for semi-finishing turning operation was used in wet lubricating conditions. The comparison between the two CoCrMo alloys machinability is presented in terms of tool wear, surface integrity and microstructural alteration.

Selection and peer-review under responsibility of the International Scientific Committee of the 6th CIRP International Conference on High Performance Cutting
doi:10.1016/j.procir.2014.03.082

2. Experimental

2.1. Materials

The materials object of the investigation are two CoCrMo alloys, one wrought and one obtained from EBM forming, with a very similar chemical composition, as it can be seen in Table 1. The wrought alloy is the ASTM F1537, being a cast ASTM F75 alloy modified through a thermo-mechanical process. The alloy structure consists of a cobalt-rich matrix (alpha phase) plus interdendritic and grain-boundary carbides $M_{23}C_6$ carbides, as shown in Fig. 1 on the right.

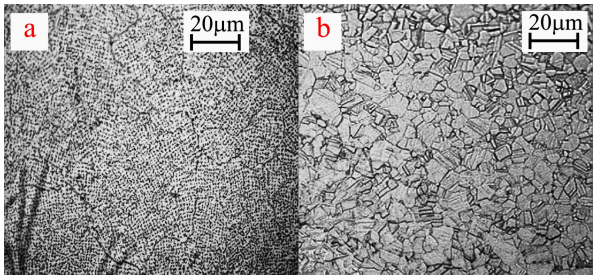

Fig. 1. Microstructure of the two CoCrMo alloys: (a) EBM; (b) wrought.

The EBM process applied on CoCrMo powders induces a strong anisotropy to the solidified material, resulting in equiaxed grains perpendicular to the building direction, and elongated grains parallel to the building direction. The microstructure of the EBM alloy, named F75, in its as-built state after the forming process perpendicular to the building direction, is shown in Fig. 1 on the left, where equiaxed grains with a massive and fine distribution of carbides both at grain boundaries and within the grains are noticeable. The as-built EBM alloy, thanks to the great amount of $M_{23}C_6$ and M_6C carbides, is reasonably supposed to be more difficult to machine than the wrought alloy. The main mechanical properties of the two alloys are reported in Table 2.

Table 1. Chemical composition of the two CoCrMo alloys (% in weight).

Material	C	Cr	Mo	Ni	Fe	Si	Mn	Co
ASTM F1537	≤0.14	26-30	5-7	1 max	0.75	1max	1max	balance
ASTM F75EBM	≤0.14	27-30	5-7	<0.5	<0.75	<1%	<1%	balance

Table 2. Mechanical properties of the two CoCrMo alloys.

Property		as-built F75	wrought F1537
Elastic Modulus	[GPa]	165	240
Hardness	[HRC]	47	35
UTS	[MPa]	719	1172
Yield Strength	[MPa]	796	827
Elongation	[%]	1.0	12

2.2 Machining Tests

The machining tests were conducted on a Mori Seiki NL 1500™ CNC lathe with the goal of investigating and comparing the machinability of two CoCrMo alloys. A 5% mineral oil and water emulsion, supplied at 6 bars, was applied in the cutting area realising a fully lubricated condition. In the case of the wrought alloy, the test specimens were obtained from a 29 mm diameter round bar and 300 mm long pieces were cut, while for the EBM alloy, the as-built bar was 50 mm diameter and 150 mm long pieces were cut. Before realising the turning operations, a 2 mm width surface was removed in order to eliminate surface defects, and the porous and abrasive layer in the case of the EBM alloy. The cutting tool used in the tests was the semi-finishing coated tungsten carbide insert CNMG120404SM-GC1105 supplied by Sandvik-Coromant. The selected insert grade GC1105 is characterized by a fine grain WC substrate, which gives good heat and plastic deformation resistance; the coating consists of a TiAlN layer deposed by PVD, which allows good toughness, uniform flank wear, and overall high machining performances. The tool radius was 0.4 mm, the rake and clearance angles were respectively 7° and 0° with chip breaker, the adopted tool holder was a Sandvik PCLNR/L with an approach angle Kr of 75°. Since very few works can be found in literature concerning experimental studies on the machinability of CoCrMo alloys, as well as very few technical references are in general available, the adopted cutting parameters for both the alloys followed the recommendations of the tool manufacturer to machine wrought CoCrMo alloys. Even though the adopted cutting parameters could not represent the optimal solution to machine the EBM alloy, nevertheless they permit a robust comparison between the behaviour of the two alloys, pointing out the effect of the forming process on the subsequent machinability. Two values of the cutting speed and of the feed rate were chosen, namely 40 and 60 mm/s, and 0.1 and 0.15 mm/rev, respectively; the depth of cut was kept constant and equal to 0.1 mm. The turning tests were conducted at fixed time length of 3-8-15 minutes for each cutting condition, adopting a single cutting edge for each trial. At the end of each turning step, a 20 mm long specimen was cut from the bar, as well as the turning inserts and the chips were collected to carry out further investigations. The tool wear was measured by means of a digital portable microscope DINOLITE AM4113ZT-X™ for a macro scale analysis and a FEI QUANTA 450™ scanning electron microscope for a micro scale analysis. The effects of the turning parameters on the surface integrity were investigated by means of a Taylor Hobson-Subtronic 25™ portable roughness tester for measuring the R_a and R_{sm} parameters, while the surface topography scanning was performed with a Sensofar Plu-Neox™ digital profilometer with a resolution of less than 20 nm on the optical Z-axis. In order to evaluate the influence of the cutting parameters on the material structure, micro-hardness measurements were performed by means of a Leitz Durimet™ micro-hardness tester with a load of 50 gr for 30 s. The alloy microstructure was analysed after polishing and etching: a chemical etchant was adopted for the wrought alloy, while an electrochemical etching was applied to the EBM alloy. The microstructure observations were conducted using an inverted optical microscope Leica MEF4U™ equipped with a high definition digital camera.

3. Results

3.1. Wear Behavior

Table 3. Tool wear at different cutting times and parameters for the two CoCrMo alloys (in red the tool life criterion is reached).

Material	Cutting parameters				Cutting time [min]
	V_c 40 m/min f 0.1 mm/rev	**V_c 60 m/min f 0.1 mm/rev**	**V_c 40 m/min f 0.15 mm/rev**	**V_c 60 m/min f 0.15mm/rev**	
ASTM F1537 Wrought CoCrMo	FW, CP Vb_c=0.05 mm	FW, NW Vb_c=0.47 mm Vb_N=0.09 mm	FW, NW, CH, BUL Vb_c=0.07 mm Vb_N=0.08 mm	FW, CP, CH, BUL Vb_c=0.09 mm Vb_N=0.12 mm	**3**
	FW, CEFD Vb_c=0.13 mm	FW, NW, CP, BUL Vb_c=0.06 mm Vb_N=0.1 mm	FW, CP, NW, BUL Vb_c=0.14 mm Vb_N=0.16 mm	CP, CH, NW, BUL Vb_c=0.15 mm Vb_N=0.18 mm	**8**
	FW, CP, CEFD Vb_c= 0.18 mm	FW, NW, CEFD, BUL Vb_c=0.15 mm Vb_N=0.13 mm	NW, CP, CEFD, BUL Vb_c=0.19 mm Vb_N=0.22 mm	SNW, SCP, BUL Vb_c=0.21 mm Vb_N=0.21 mm	**15**
ASTM F75 EBM CoCrMo	AB, FW Vb_c=0.04 mm	SCP, CR, BUE	SER, AB, NW	SCR, AB, ER, FW	**3**
	CP, CR, FW Vb_c=0.055 mm	SAB, BUE, CR, RFC	SER, SAB, CR	RFC, FL, SER, SAB, CR	**8**
	ER, CR, BUE	SER, CR, RFC	SER, SAB, SCFED	CF	**15**

FW: flank wear, **CP:** cutting edge chipping, **NW:** notch wear, **CEFD:** cutting edge fragment detachment, **SNW:** severe notch wear, **CR:** cratering **SCP:** severe cutting edge chipping, **BUE:** built up edge, **SCEFD:** severe cutting edge fragment detachment, **RFC:** rake face cracking, **BUL:** built up layer, **AB:** abrasion, **ER:** erosion, **SCR:** severe cratering, **SER:** severe erosion, **SAB:** severe abrasion, **FL:** flaking, **CF:** catastrophic failure.

Several tool wear mechanisms were observed in turning the wrought and EBM CoCrMo alloys: the same aspect was observed also on other superalloys, such as the Inconel 718 and Ti6Al4V as found in [3,4]. For each turning step, these mechanisms did not exhibit individually, therefore different tool wear criteria had to be defined in order to establish the state of the cutting tool and a rejection condition. The flank wear parameter VB_c under the tool tip and the notch wear parameter VB_N were measured following the ISO3685 standard [5]; the SEM analysis permitted the observation of the cutting edge state, namely the presence of chipping, adhesion, cratering, BUE, fractures and catastrophic failures.

The following criteria were chosen for tool rejection:

- Maximum flank wear: Vb_c = 0.3 mm
- Maximum notch wear: Vb_N = 0.3 mm
- Fracture or catastrophic failure of the cutting tool

The evolution of the tool wear for both the materials and for all the conditions is summarized in Table 3. For each turning step, the main observed wear mechanisms are indicated, and in those cases where flank and notch wear phenomena occurred the quantitative values are presented. When at least one of the tool rejection criteria was reached, the corresponding condition was highlighted. SEM and EDS analysis showed a presence of workpiece material adhered on the tool cutting edge and rake face for all the turning condition tested and time length on the wrought alloy, as shown in Fig. 2, where the tool cutting edge is shown after 3 and 8 minutes turning under the same cutting conditions.

Notching and chipping of the cutting edge resulted the most significant wear mechanism modes observed for the wrought alloy. None of the tested cutting condition resulted in reaching the tool wear criteria, and flank wear resulted to be a secondary wear mechanism.

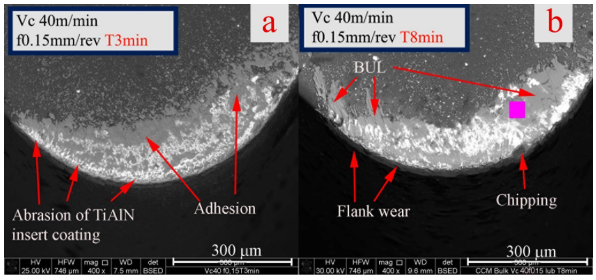

Fig. 2. SEM images of worn tools when turning wrought CoCrMo alloy after (a) 3 minutes, and (b) 8 minutes.

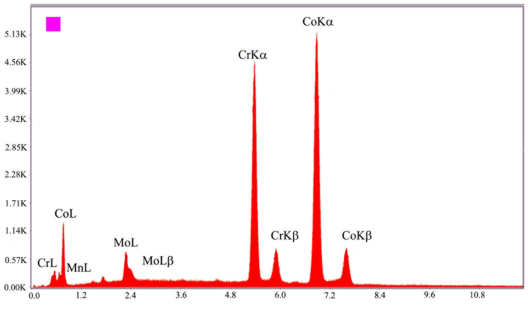

Fig. 3. EDS analysis to identify the BUL chemical composition referring to Fig. 2.

Notching at the tool tip and depth of cut was observed for three of the four cutting conditions since the first turning stages, whereas the adoption of a cutting speed of 40 m/min and a feed rate of 0.1 mm/rev resulted to minimize the notch wear. The notch formation can be attributed to the high strain hardening of the workpiece [3], high strength and abrasive chips. The cutting edge chipping is related to the attrition wear, mainly caused by the irregular flow of the work material against the cutting edge, and by the chip segmentation inducing variable forces during the process. The workpiece material adhesion tends to promote the cutting edge chipping, since the adhered material is not completely stable and can unpredictably break, tearing off a fragment of the cutting edge. To limit the cutting speed to 40 m/min resulted in increasing the cutting edge chipping since the beginning of the process, but less notch wear was observed. At a feed rate of 0.15 mm/rev, the flank wear increased as so for notch wear and chip hammering at 3 minutes of turning, while at 15 min more Cutting edge fragment detachments (Cefd) were observed due to the increased cutting forces on the tool tip.

The EBM alloy resulted to be more abrasive and less machinable than the wrought one, having reached the tool life criteria for three of the four cutting conditions; the only cutting condition that allowed reaching a turning length suitable for industrial applications is the one utilising a cutting speed of 40 m/min and a feed rate of 0.1 mm/rev. Abrasion represented the main tool wear mechanism; for all the cutting conditions, the tool coating was completely scraped from the rake face after 3 minutes of turning. Large white areas on the rake face of the insert shown in the SEM images confirmed the rubbing effect of the tool material on the TiAlN insert coating (Fig. 4). The microstructure of the EBM alloy characterized by a great amount of hard particles makes it more abrasive than the traditional wrought alloy.

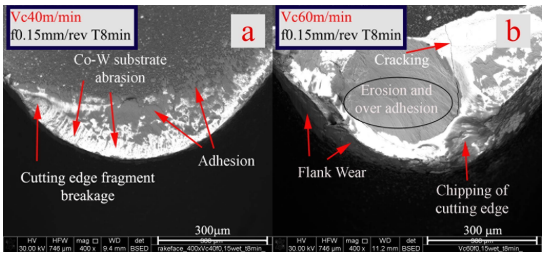

Fig. 4. SEM images showing the effects on tool wear in turning EBM alloy by adopting a cutting speed of (a) 40m/min, and (b) 60m/min.

The cutting speed influenced the formation of the crater wear at 3 minutes: a major heat generation induced by the rubbing effect at 60 m/min is supposed to induce higher chemical affinity between the workpiece and cutting tool materials and therefore tendency to crater formation. At 8 minutes, severe erosion and cratering was observed along the cutting edge, see Fig. 4, and at a feed rate of 0.1 mm/rev the BUE formation was observed. Increasing the feed rate, severe erosion is registered at 8 minutes, cracking and cratering, leading to catastrophic failure at 15 minutes. A reasonable strategy could be to try coated inserts with a harder grade testing higher parameters to increase the cutting temperature.

3.2. Surface Integrity

The surface integrity of machined surfaces is commonly characterized measuring the surface roughness parameter R_a, as well as other parameters defined according to the ISO 4287 – 1997[6] standard. In the last few years, digital optical profilometers were also adopted to analyse the effects of the cutting parameters, cutting tool geometries and different cooling strategies on the machined surface quality. 3D images of the machined surface of both the wrought and EBM alloys after 8 minutes turning are presented in Fig. 5, where the values of R_a and R_{sm} measured with a portable roughness tester are also reported.

The turned surfaces of the wrought alloy do not show surface irregularities between the feed marks that could be due to deposition of the workpiece material from adhered layers on the insert cutting edge and rake face , as found in [7] in dry turning of Inconel 718 for similar cutting conditions. Even though a great amount of the workpiece material adhered on the insert rake face was observed, see Fig. 2 and 3, loose arc chips and low flank wear reduced the removing of material fragments from the Build Up Layers (BUL) and deposition on the machined surfaces. Material side flow and plastic deformation along the feed marks can be observed for all the cutting conditions after 8 min turning, and similar results were observed after 3 and 15 minutes. According to [8], material side flow occurs when the chip thickness is lower than a minimum chip thickness that depends on the workpiece material, cutting conditions, micro and macro geometry of the cutting tool. When this condition occurs, the material in the feed mark area is squeezed, ploughed and deformed plastically aside leaving these double feed marks. Chipping and notching of the cutting edge since the first minutes of turning facilitated this phenomenon, and the material being plastically deformed filled the grooves present along the cutting edge. The measured surface roughness values are mainly influenced by the feed rate: for all the turning times the average values are incremented of more than 50% by increasing the feed rate from 0.1 to 0.15 mm/rev. The tool wear effect on the surface roughness was not been sensible for the three turning time. For all the cases, a R_a reduction was measured from 3 to 8 minutes, this can be attributed to the low abrasion occurred on tool flank face and to the greater amount of workpiece material adhered on the cutting edge that played a protection role against abrasive wear. The increase in the cutting speed induced a sensible reduction of R_a at 3 and 8 minutes for a feed rate of 0.1mm/rev, which can be attributed to higher cutting edge chipping at lower cutting speed, while for a feed rate of 0.15 m/rev higher flank wear and chipping induced an R_a increase since the very beginning of the turning process.

3D images of the EBM alloy machined surfaces confirm the results about the tool wear comparison between the two alloys. Even though at the first stages of turning, the EBM alloy R_a values are comparable to those of the wrought alloy, several craters, laps and cracks are present on the machined surfaces between and across the feed marks, making the surface quality not ideal for biomedical applications, where fretting, fatigue and tribo-corrosion resistances are required.

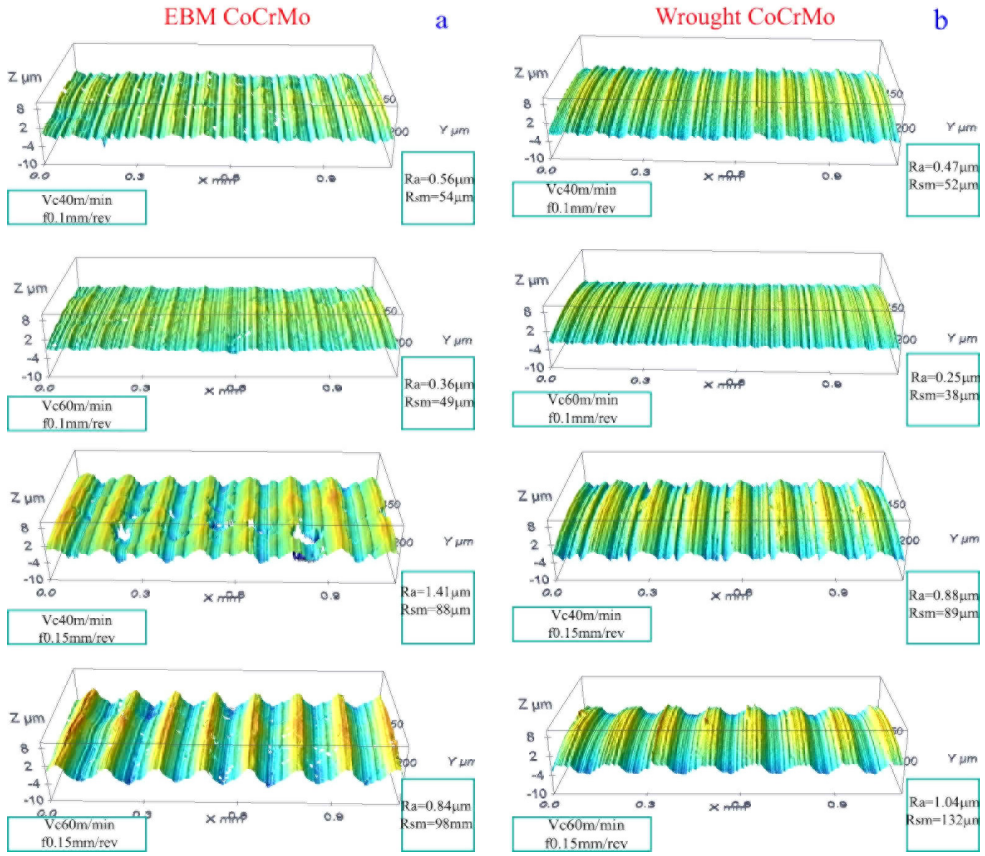

Fig. 5. Comparison between the surface topographies adopting different cutting parameters after 8 minutes of turning : (a) EBM alloy, and (b) wrought alloy.

These surface macro defects tends to increase at increasing feed rate, and even a crater of 0.11 mm width and 15 µm depth was measured. Such kind of defects can be caused by the chip formation mechanism, which is not characterized by plastic flow on the primary shearing zone on the insert rake face. The chip morphology obtained for all cutting conditions and for different turning times didn't changed significantly, and chips in form of powder particles were collected. The chips did not undergo any plastic deformation, leading to brittle fracture, and resulting in the formation of a crater. At increasing feed rate to 0.15 mm/rev, the surface roughness increased more than 50% at 15 min of turning compared to the values measured on the wrought alloy. Material side flow and plastic deformation can be observed on the scanned surfaces as for the wrought alloy, no substantial variations were registered in the other time steps, but in the case of the EBM alloy this kind of defects can be considered of secondary importance.

3.3 Micro-hardness and microstructure

The wrought and EBM CoCrMo alloys present different microstructures induced by the previous forming process. Tool wear and surface integrity analyses has revealed that the machinability of the EBM alloy is much lower than the wrought one, with a tool life reduced to less than ten minutes, and the machined surface is full of wide and deep craters. In Fig. 6 and 7, the micro-hardness profiles under the turned surface in the radial direction after 8 minutes turning are presented. Both the wrought and EBM alloys show a gradient in the micro-hardness profiles. Increasing cutting speed and feed rate, an increase in the micro-hardness was observed for both the alloys, which can be attributed to higher thermal and mechanical load on the material surface raising the strain hardening effect. The condition that provoked the higher hardening effects on the surface layer was obtained at the maximum cutting speed and feed rate: this could be attributed to the higher tool wear, the tool tip resulted more chamfered than in the other cutting conditions, provoking more generation of heat due to abrasion, therefore more temperature increase and strain hardening effects.

Even if the EBM alloy values of micro-hardness were higher than the wrought alloy ones, the EBM alloy showed a ratio between the surface and the bulk hardness comparable to that of the wrought material; in fact, on an average, a 30% micro-hardness increase was measured from the bulk to the surface for both the alloys. An example of the sub-surface microstructure for both the alloys is shown in Fig. 8. The wrought alloy presents a 150 µm width sub-surface layer, affected by grain refinement and grain deformation along the

cutting speed direction (Fig. 8 lower part). The EBM alloy presents a deformed layer as well (Fig. 8 upper part), and the zoomed snapshot shows the deformed grain boundaries along the turned surface: this trend was observed for all the cutting conditions at 8 and 15 minutes, while at 3 minutes the tool wear did not make the grain boundaries to be deformed along cutting direction.

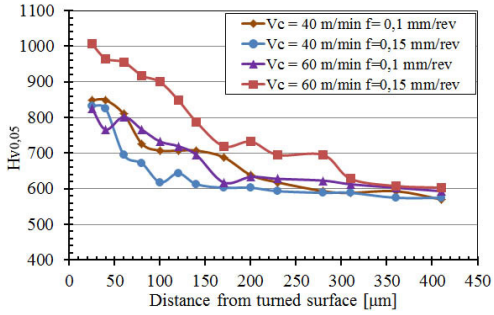

Fig.6. EBM alloy micro-hardness as a function of the cutting parameters.

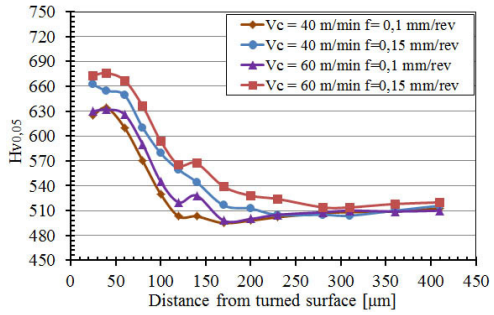

Fig. 7. Wrought alloy micro-hardness as a function of the cutting parameters.

4. Conclusions

The paper presented the results of an experimental campaign aimed at investigating and comparing the machinability characteristics of two CoCrMo superalloys, one wrought and the other additive manufactured by Electron Beam Melting. Surface integrity, tool wear and material microstructure alteration were analysed, and the effects of cutting parameters were tested. The main outcomes can be summarized as follows:

- Tool wear when turning the wrought alloy is characterized by adhesion, chipping and notch wear for all the cutting conditions. BUL formation is observed at the first stages of turning, while cutting edge fragments detachments is observed at 15 minutes.
- The EBM alloy is more abrasive than wrought alloy: the adoption of a cutting speed of 40 m/min and a feed rate of 0.1 mm/rev did not cause the reaching of the tool life criteria at 8 and 15 min as it happened when adopting more severe cutting conditions. The increase in the cutting speed and feed rate resulted in severe erosion, abrasion, cratering and in some cases cracking at 8 minutes of turning.
- The surface integrity is better for the wrought alloy, even though comparable values of R_a are measured: the EBM alloy presents macro-scale craters on the turned surface, which tend to increase at increasing the cutting parameters. Both alloys showed material side flow and plastic deformation in the area of the feed marks.
- The effect of the turning process resulted in a deformed sub-surface layer along the cutting direction, and in the case of the wrought material a grain refinement is appreciable. The strain hardening induced a surface hardening of the material with a radial gradient, which increases at increasing the cutting parameters.

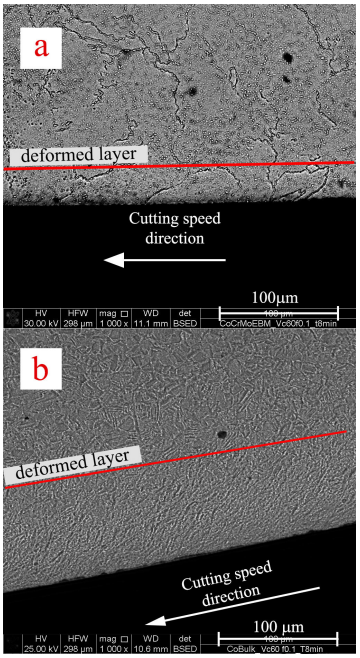

Fig. 8. Effect of turning on the sub-surface microstructure of: (a) EBM alloy, and (b) wrought alloy at 8 minutes of turning.

References

[1] Shao H. Study on machinability of a stellite alloy with uncoated and coated carbide tools in turning. J Manuf Process (2013), http://dx.doi.org/10.1016/j.jmapro.2013.10.001.
[2] Deshpande A. Machining of CoCrMo Alloys for Reduced Wear Debris Generation in Metal-on-metal Hip Implants. PhD Dissertation 2010, University of Kentucky.
[3] Cantero JL, Dìaz-Alvarez J, Miguelez MH, Marin NC, Analysis of tool wear patterns in finishing turning of Inconel 718. Wear 297 (2013) 885–894.
[4] Armendia M, Garay A, Iriarte LM, Arrazola PJ. Comparison of the machinabilities of Ti6Al4V and TIMETAL®54M using uncoatedWC–Co tools. Journal of Materials Processing Technology210 (2010) 197–203.
[5] ISO 3685, Tool life testing with single-point turning tools, 1993.
[6] ISO 4287, Geometrical Product Specifications (GPS) Surface texture: Profile method,Terms, definitions and surface texture parameters,
[7] Devillez A, Le Coz G, Dominiak S, Dudzinski D. Dry machining of Inconel 718, workpiece surface integrity. Journal of Materials Processing Technology 211 (2011) 1590– 1598.
[8] Kishway HA, Elbestawi MA. Effects of process parameters on material side flow during hard turning. International Journal of Machine Tools and Manufacture 39 (7), 1017–1030.